Competitive occurrence of homolytic N–O and heterolytic C–O bond cleavage in excited-state 1-(arylmethyloxy)-2-pyridones

Nariyoshi Yoshioka,[a] Chihei Andoh,[a] Kanji Kubo,[b] Tetsutaro Igarashi[a] and Tadamitsu Sakurai *[a]

[a] *Department of Applied Chemistry, Faculty of Engineering, Kanagawa University, Kanagawa-ku, Yokohama, 221-8686, Japan*
[b] *Institute of Advanced Material Study, 86, Kyushu University, Kasuga-koen, Kasuga, Fukuoka 816-0811, Japan*

Received (in Cambridge, UK) 4th June 2001, Accepted 16th July 2001
First published as an Advance Article on the web 4th September 2001

The irradiation at 340 nm of the title compounds having 9-anthryl and pyren-1-yl groups in methanol was found to give the heterolytic C–O bond cleavage products: 1-hydroxy-2-pyridone and aryl-substituted dimethyl ether (which predominate for the reaction of the former title compound) in addition to 2-pyridone, aryl-substituted methanol and aryl-substituted formaldehyde derived from the homolysis of the N–O bond (which mainly occurs in the photolysis of the latter title compound). It was also found that substitution of the methyl group for hydrogen at the 6-position of the pyridone skeleton in 1-(9-anthrylmethyloxy)-2-pyridone decreases the relative composition of the aryl-substituted dimethyl ether to some extent. These substituent effects on the product compositions were explained in terms of stereoelectronic effects on a charge transfer-type interaction between the aromatic and pyridone rings in the singlet excited state. Analyses of the ground-state conformation for the title compounds by MM2 calculations and ^{1}H NMR spectroscopy, as well as of their singlet excited-state behaviour, substantiated the existence of a non-emissive intramolecular exciplex intermediate which plays a key role in inducing the C–O bond heterolysis.

Introduction

Photochemistry has continued to contribute to the development of efficient and selective transformations of organic compounds into functional materials such as photoinitiators, light energy-storage polymers and plastic optical fibres. Recently, photochemical control of the homolytic *versus* heterolytic bond-cleavage pathway has been the subject of extensive research efforts[1–5] because of its potential application to developing protecting groups of biological molecules[1,2] as well as photoinitiators with high selectivities.[3] Through comprehensive mechanistic studies on the photolysis of arylmethyl esters in nucleophilic solvents, Pincock and his co-workers have shown that the dominant primary step is homolytic C–O bond cleavage from the singlet excited state to form a radical pair, electron transfer in which eventually gives an ion-derived product along with a radical-derived one.[4] However, there is no study regarding the possibility of heterolytic bond cleavage induced by the formation of an intramolecular exciplex with some charge-transfer character.

In the course of our systematic study toward the characterization of the excited-state behaviour of cyclic hydroxamic acid derivatives, we found that bichromophoric 1-benzyloxy-2-pyridone in the singlet excited state undergoes homolytic N–O bond cleavage exclusively, giving benzaldehyde and 2-pyridone as major products along with a minor amount of benzyl alcohol.[6] In addition, internal and external heavy-atom effects on the emission intensity and the quantum yield for disappearance of the starting 2-pyridone derivative indicated that the homolysis of the N–O bond takes place from a hot vibrational level of the first singlet excited state. It was also shown (through analyses of the ground-state conformations for 1-benzyloxy-2-pyridone and related compounds, as well as of the deuterium isotope effects on the quantum yield) that the reaction proceeds mainly through a folded conformation but not a stretched one.[7] Thus, the previous findings described above allow us to expect that the replacement of the phenyl group in our bichromophoric molecule by the anthryl or the pyren-1-yl group would substantially enhance a charge transfer-type interaction between the two chromophores in the singlet excited state, affecting the bond-fission process of these *O*-substituted cyclic hydroxamic acids. In order to explore the possibility of photochemical control of heterolytic *versus* homolytic bond scission in bichromophoric 1-hydroxy-2-pyridone derivatives having a 9-anthryl or a pyren-1-yl pendant, we designed and synthesized 1-(9-anthrylmethyloxy)-2-pyridone (**1a**), 1-(9-anthrylmethyloxy)-6-methyl-2-pyridone (**1b**) and 1-(pyren-1-ylmethyloxy)-2-pyridone (**1c**). In this paper we present results which demonstrate that bichromophoric 1-(arylmethyloxy)-2-pyridones having a strong ability to form an exciplex intermediate undergo novel heterolytic cleavage of the C–O bond in competition with the homolysis of the N–O bond in their singlet excited states.

Results and discussion

Products and their composition analysis

On irradiation of a nitrogen-purged methanol solution of **1a** (1.0×10^{-3} mol dm^{-3}) with light of wavelength longer than 340 nm (from a 450 W high-pressure Hg lamp) at room temperature, there appeared four new HPLC signals with retention times of 4.5 (1-hydroxy-2-pyridone **2a** and 2-pyridone **3a**), 9.5 (anthracene-9-methanol **4a**), 21.9 (anthracene-9-carbaldehyde **5a**) and 28.5 min [9-(methoxymethyl)anthracene **6a**], in addition to that of the starting **1a** (retention time: 13.5 min) (Scheme 1). Each product was identified by comparing its HPLC behaviour with that of the corresponding authentic sample under several analytical conditions. Since the unexpected product **6a** as well as the substantial overlap of HPLC signals for **2a** and **3a** had been observed, we attempted

DOI: 10.1039/b104849j

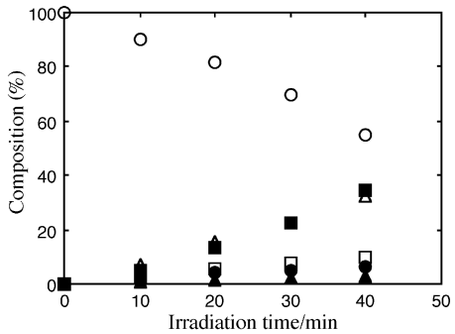

Fig. 1 Relation between irradiation time and composition of each compound in methanol. ○: **1a**, △: **2a**, □: **3a**, ●: **4a**, ▲: **5a** and ■: **6a**.

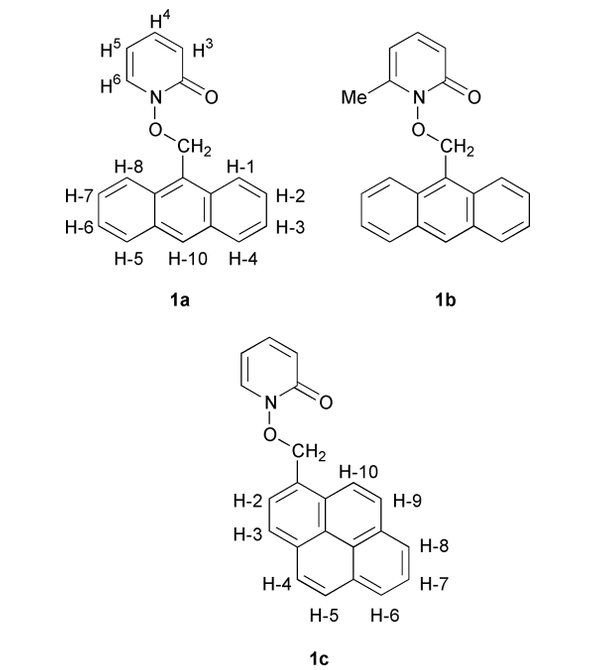

Scheme 1 Product distribution in the photolysis of **1a**–**c**.

to isolate these products by preparative thin layer chromatography over silica gel and succeeded in obtaining **6a** in 25% yield (conversion: 45%) along with a mixture of **2a** and **3a** whose ^{1}H NMR spectrum was compatible with that of a mixture of authentic **2a** and **3a**. As demonstrated in Fig. 1, the composition of **2a** (major) is comparable to that of the ether **6a** at each irradiation time, while the same relation holds among the compositions of **3a** (minor), the alcohol **4a** and the aldehyde **5a**, namely **3a** ≈ **4a** + **5a**. For example, the 30 min irradiation of **1a** (1.0×10^{-3} mol dm^{-3}) in methanol gave **2a** (composition: 22.9%), **3a** (8.3%), **4a** (6.0%), **5a** (2.8%) and **6a** (22.4%) at 31.2% conversion of the starting **1a**. Since arylmethyl carbonium ions readily react with methanol giving the corresponding arylmethyl methyl ether,[4] this observation suggests that the ether **6a** is derived from heterolytic C–O bond cleavage in **1a** but not from the homolytic N–O bond scission which should be responsible for the appearance of **3a**, **4a** and

Table 1 Chemical shifts (δ) of the pyridone-ring protons for 1-ethoxy-2-pyridone (R = Me), **1a** (R = 9-anthryl) and **1c** (R = pyren-1-yl) in $CDCl_3$ at 24 °C

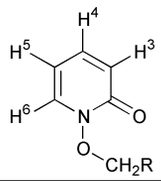

R	H^3	H^4	H^5	H^6
Methyl	6.66	7.33	6.15	7.55
9-Anthryl	6.71	7.17	5.72	6.92
Pyren-1-yl	6.72	7.18	5.67	6.87

5a.[6] Additional evidence for the existence of a 9-anthrylmethylcarbonium ion intermediate comes from the observation that the irradiation of **1a** (1.0×10^{-3} mol dm^{-3}) in ethanol affords 9-(ethoxymethyl)anthracene (composition: 7.0%) along with **4a** (4.6%) and **5a** (1.8%) under the same irradiation conditions (conversion: 13.4%, HPLC analysis). The less polar protic solvent is considered to inhibit the heterolysis of the C–O bond to some extent and also to lower the photoreactivity of the starting **1a**.

Similar product distribution and composition (**4a**, 6.0%; **5a**, 7.0%; **6a**, 12.7%) were obtained by the irradiation of **1b** (1.0×10^{-3} mol dm^{-3}) in methanol under the same conditions (conversion: 25.7%, HPLC analysis) (Scheme 1). Because no HPLC signals other than those of **1b**, **2b** + **3b**, **4a**, **5a** and **6a** could be detected on the chromatogram, the reaction of **1b** should also proceed without any detectable formation of by-products to give **2b**, the composition of which must be compatible with that of the ether **6a**. A comparison of the relative composition of **6a** derived from the photolysis of **1a** (72%) and **1b** (49%) confirms that the substitution of the methyl group for hydrogen at the 6-position of the pyridone skeleton decreases this relative composition to some extent, suggesting that the methyl group exerts its stereoelectronic effect on the heterolytic C–O bond cleavage process.

On the other hand, the irradiation of **1c** (5.0×10^{-4} mol dm^{-3}) in methanol under the same reaction conditions as those used for **1a** and **1b** afforded **2a** (composition: 5.0%), **3a** (19.4%), **4c** (3.0%), **5c** (17.3%) and **6c** (4.1%) at 24.4% conversion of the starting **1c** (^{1}H NMR analysis, Scheme 1). Evidently, the introduction of the pyren-1-yl group instead of the 9-anthryl into **1** renders the heterolytic C–O bond cleavage a minor pathway. The large difference in composition for the ion-derived products between **1a** and **1c** may argue against a mechanism involving initial homolysis of the C–O bond, followed by electron transfer.[4,5]

Conformational analysis and fluorescence quenching

In order to probe the interesting substituent effects on the product composition, we analyzed the ground-state conformation by means of ^{1}H NMR spectroscopy and MM2 calculations. An examination of Table 1 reveals that the replacement of the ethyl substituent in 1-ethoxy-2-pyridone by the 9-anthrylmethyl (**1a**) or the pyren-1-ylmethyl (**1c**) results in a relatively large upfield shift of the pyridone-ring proton H^5 and H^6 signals. Taking into account that this upfield shift is due to aromatic ring-current effects,[7] we are led to propose a folded conformation which is substantiated by the corresponding energy-minimized conformation (MM2 calculations), as shown in Fig. 2. Additional evidence for the folded conformation comes from an analysis of the NOESY spectrum of **1** in [^{2}H]chloroform ($CDCl_3$), typically depicted in Fig. 3. The analysis indicates that there are relatively strong cross peaks between the pyridone-ring proton H^6 signal and the

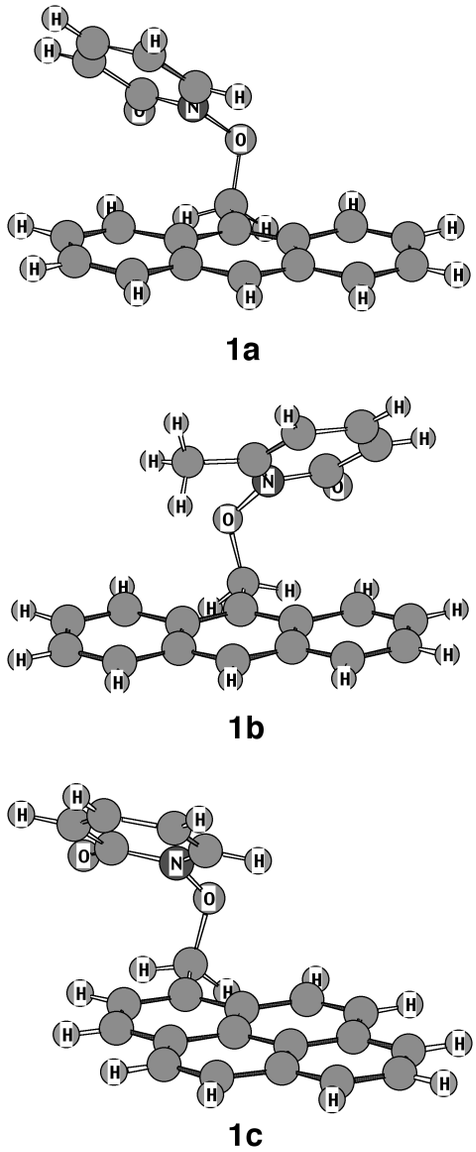

Fig. 2 Energy-minimized conformations of **1a**, **1b** and **1c**.

anthracene-ring proton H-1 (or H-8) and H-2 (or H-7) signals in **1a**, while the H^5 signal also correlates less strongly with the H-2. Similar correlations were observed between the pyridone-ring Me^6 proton signal and the H-1 and H-10 signals in **1b**. Although unambiguous assignment of all the pyrene-ring proton signals in **1c** was impossible to make from its 2D NMR analysis, both the H^5 and H^6 signals were found to correlate weakly with the pyrene-ring H-9 and H-10 (or H-2 and H-3) signals. It is, thus, expected that there is appreciable interaction between the pyridone and aromatic rings in the ground state and also in the singlet excited state.

As we expect, the first absorption band (arising from the anthracene ring of **1a**) was red-shifted by 12 nm with broadening of each vibrational structure, as compared to that of the reference compound, anthracene (the first singlet excitation energy, $E_S = 319$ kJ mol^{-1}; the first triplet excitation energy, $E_T = 178$ kJ mol^{-1})[8] (Fig. 4). In addition, we observed intramolecular fluorescence quenching of the anthracene chromophore by the pyridone having excitation energies of 343 (E_S)[6] and 268 kJ mol^{-1} (E_T)[6] (Fig. 5). Almost the same absorption and emission behaviour was observed also for **1b** and anthracene. Interestingly, the extent of the fluorescence quenching of the pyrene chromophore in a **1c** molecule is much smaller than that of the anthracene in **1a** and **1b** (Fig. 6), whereas the first absorption band of **1c** is shifted to longer wavelength by 10 nm, compared

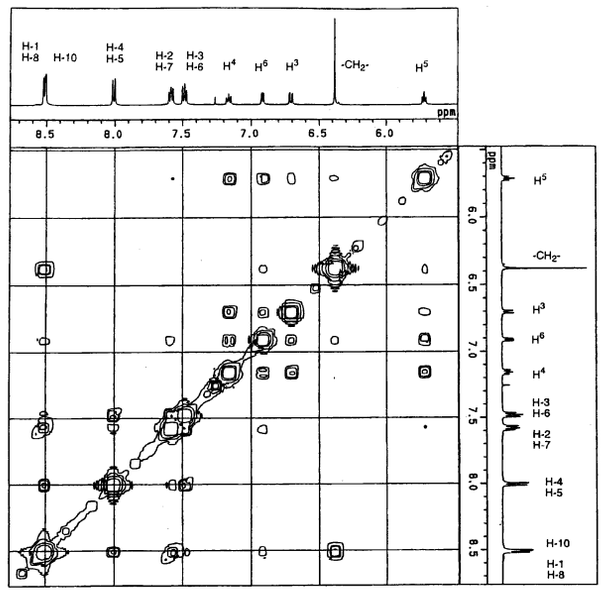

Fig. 3 NOESY spectrum of **1a** in [^{2}H]chloroform at 24 °C.

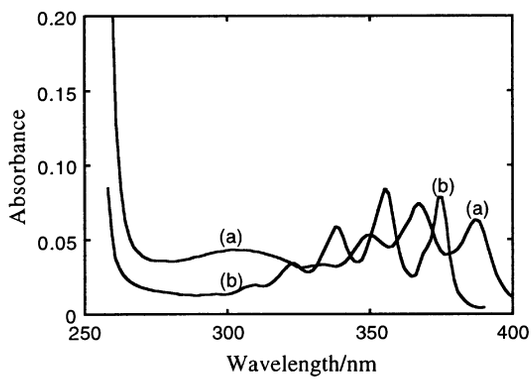

Fig. 4 UV absorption spectra of **1a** (curve a, 0.7×10^{-5} mol dm^{-3}) and anthracene (curve b, 1.0×10^{-5} mol dm^{-3}) in methanol at room temperature.

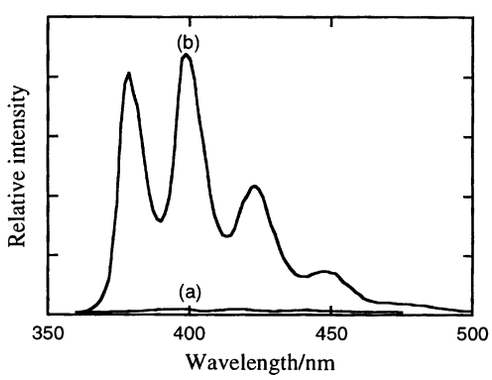

Fig. 5 Fluorescence spectra of **1a** (curve a, 0.7×10^{-5} mol dm^{-3}) and anthracene (curve b, 1.0×10^{-5} mol dm^{-3}) in nitrogen-saturated methanol at room temperature. Excitation wavelength is 342 nm.

with that of its reference, pyrene ($E_S = 321$ kJ mol^{-1}; $E_T = 202$ kJ mol^{-1})[8] (Fig. 7). The finding of endothermic energy transfer from the anthracene or the pyrene moiety (that is selectively excited) to the pyridone in **1** strongly suggests the involvement of a non-emissive intramolecular exciplex with some charge-transfer character as a precursor of the heterolytic C–O bond cleavage products **2** and **6** (Scheme 2). The suggestion described above is substantiated by the occurrence of intramolecular

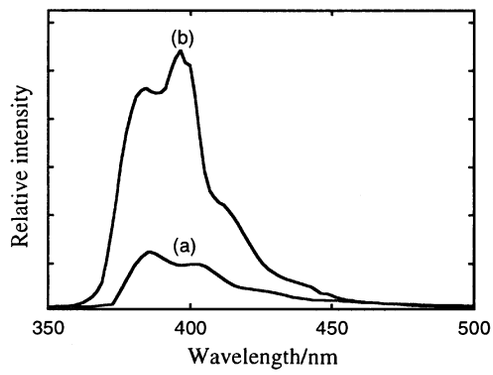

Fig. 6 Fluorescence spectra of **1c** (curve a, 1.5×10^{-6} mol dm^{-3}) and pyrene (curve b, 1.5×10^{-6} mol dm^{-3}) in nitrogen-saturated methanol at room temperature. Excitation wavelength is 336 nm.

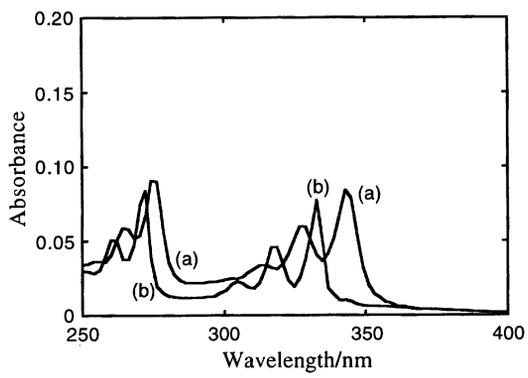

Fig. 7 UV absorption spectra of **1c** (curve a, 1.5×10^{-6} mol dm^{-3}) and pyrene (curve b, 1.5×10^{-6} mol dm^{-3}) in methanol at room temperature.

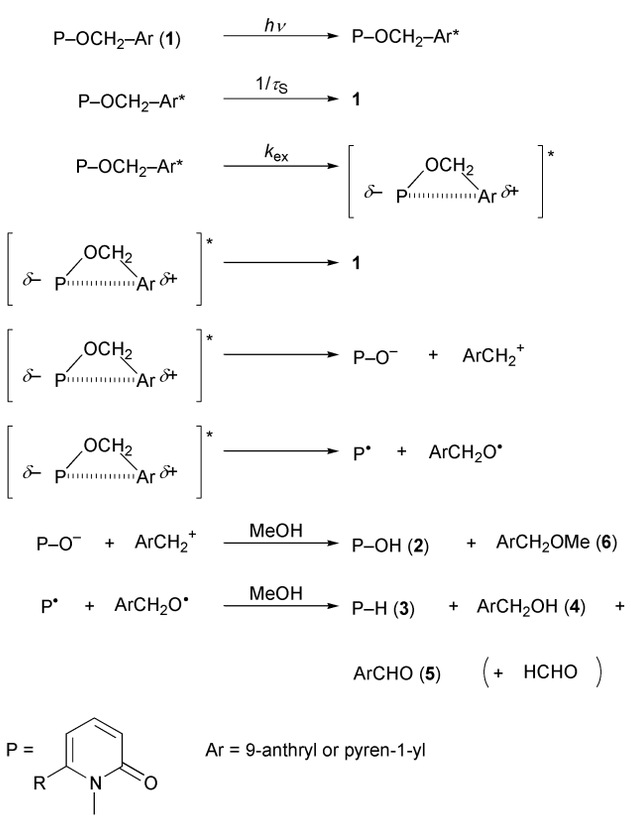

Scheme 2 Reaction mechanism for the photolysis of **1** in methanol.

charge-transfer deactivation of the excited 9-anthryl chromophore by the propiophenone moiety in ω-(9-anthryl)propiophenones.[9] Further evidence for the involvement of the exciplex

Table 2 Quantum yields of the formation of **4** (Φ_4), **5** (Φ_5) and **6** (Φ_6) for the photolysis of **1a** (1.0×10^{-3} mol dm^{-3}), **1b** (1.0×10^{-3} mol dm^{-3}) and **1c** (5.0×10^{-4} mol dm^{-3}) with 366 nm light in MeOH at 24 ± 2 °C

Compound	Φ_4	Φ_5	Φ_6	R^a
1a	0.013 ± 0.002	0.008 ± 0.001	0.045 ± 0.002	0.68
1b	0.025 ± 0.003	0.015 ± 0.001	0.037 ± 0.003	0.48
1c	0.012 ± 0.001	0.068 ± 0.003	0.016 ± 0.001	0.17

^{a} $R = \Phi_6/(\Phi_4 + \Phi_5 + \Phi_6)$.

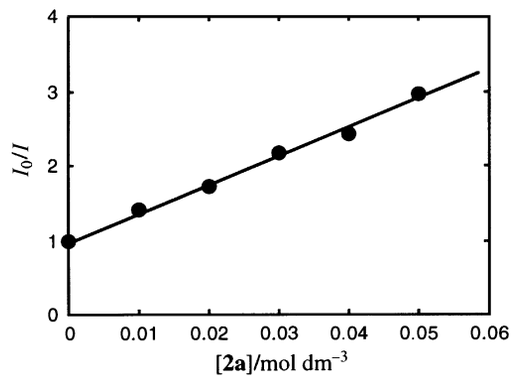

Fig. 8 Stern–Volmer plot for the fluorescence quenching of **1a** (1.0×10^{-5} mol dm^{-3}) by **2a** in nitrogen-saturated methanol at room temperature. Excitation wavelength is 366 nm.

intermediate comes from the observation that the fluorescence of anthracene is quenched by 1-hydroxy-2-pyridone (**2a**) according to the Stern–Volmer equation ($I_0/I = 1 + 38$[**2a**], where I and I_0 are the fluorescence intensities of anthracene with and without **2a**), as shown in Fig. 8. From the fluorescence lifetime of anthracene (4.2 ns) and the slope of the linear plot, the rate constant for intermolecular fluorescence quenching was determined to be 9.0×10^9 dm^3 mol^{-1} s^{-1} at room temperature. On the other hand, application of the steady-state approximation to Scheme 4 allows us to derive eqn. (1), where k_{ex} is the

$$k_{ex} = \tau_S^{-1}[(\Phi_f^0/\Phi_f) - 1] \quad (1)$$

rate constant for exciplex formation, τ_S is the fluorescence lifetime of anthracene or pyrene (91 ns) and Φ_f^0/Φ_f is the ratio of the fluorescence quantum yield of the reference to that of **1a**–**c**. Because this quantum-yield ratio can be approximated by the area ratio of their fluorescence bands, the latter ratio enabled estimation of the rate constant for exciplex formation as 3.6×10^9 (**1a**), 3.1×10^9 (**1b**) and 6.0×10^7 s^{-1} (**1c**). Comparison of these rate constants reveals that **1a** and **1b** having an anthracene ring form a much more stable non-emissive exciplex intermediate, as compared to **1c** containing a pyrene ring, whereas the methyl group in **1b** affects the exciplex-forming process to only a small extent.

Quantum yield for the reaction in methanol

In order to compare the reactivities of exciplex intermediates derived from the singlet excited-state **1a**–**c**, the quantum yields for appearance of the products **4**–**6** were determined by using a potassium tris(oxalato)ferrate(III) actinometer (Table 2),[10] whereas we could not estimate accurately the Φ value for disappearance of the starting **1** (≈ 0.1), owing to the low reaction efficiency. In addition, the quantum yield for appearance of each product was subject to, if any, only a small concentration effect in the range 0.50–2.5 × 10^{-3} (**1a**) or 0.20–1.0 × 10^{-3} mol dm^{-3} (**1c**). Table 2 clearly shows that the intramolecular exciplex intermediate (in which the aromatic and pyridone rings serve as electron donor and acceptor, respectively) does not have high reactivity. Interestingly, **1a**–**c**-derived exciplexes are similar in their reactivities, implying that a less stable

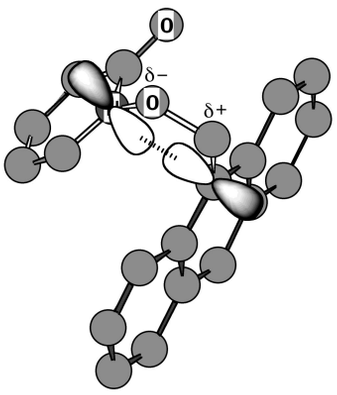

Fig. 9 Schematic illustration for the singlet-exciplex intermediate derived from **1a**.

intermediate accelerates both deactivation and bond-cleavage processes within this intermediate. We use the ratio (R) of Φ_6 to ($\Phi_4 + \Phi_5 + \Phi_6$) in order to estimate the contribution of the heterolytic C–O bond cleavage process to the overall reaction (Table 2). An examination of substituent effects on the R value confirms that the replacement of the 9-anthryl group by the pyren-1-yl group substantially decreases the contribution of the C–O bond heterolysis with an increase in the contribution of the N–O bond homolysis, whereas the methyl substituent in **1b** exerts its stereoelectronic effect so as to lower the former contribution to some extent.

Because the E_S and the oxidation potential for anthracene are nearly equal to those for pyrene,[8,11] it is very hard to interpret the observed substituent effects in terms of electron transfer (from the aromatic ring to the pyridone skeleton) within a non-emissive exciplex intermediate. Conformational analyses of the ground-state **1a**–**c** by MM2 calculations and 2D NMR spectroscopy suggest a strong charge transfer-type interaction between the 2p orbital of the amide nitrogen atom and the 2p orbital of the carbon atom at the 9-position of the anthryl group (**1a**,**b**) or the 1-position of the pyrenyl (**1c**). Thus, the fact that the heterolytic C–O bond cleavage takes place much more readily in the **1a**-derived exciplex intermediate than in the **1c**-derived exciplex leads us to assume that there is a much stronger orbital interaction within the former exciplex than in the latter to cause polarization of the C–O bond to a much larger extent, as shown in Fig. 9. This assumption is supported by the observation of the drop in contribution of the heterolytic bond-cleavage process in the less polar protic solvent, ethanol. On the other hand, a comparison of the energy-minimized conformations for **1a** and **1b** (Fig. 2) shows that the methyl substituent in the latter molecule makes the distance between the pyridone and anthracene rings somewhat longer, as compared to that in the former. Accordingly, it is reasonable to explain the decreased contribution of the C–O bond heterolysis in **1b** in terms of the charge transfer-type interaction between the two orbitals, which is weakened owing to stereoelectronic effects of the methyl group. Because the 366 nm light used for the quantum-yield measurements is able to selectively excite the 9-anthryl or the pyren-1-yl chromophore without affecting the electronic state of the pyridone moiety, the contribution of the process, P–OCH_2–Ar* $\longrightarrow$ $P^{\bullet}$ + $ArCH_2O^{\bullet}$, should be minor (Scheme 2). Therefore, we are led to conclude that the heterolytic cleavage of the C–O bond mainly occurs in competition with the homolysis of the N–O bond within the non-emissive exciplex, as already shown in Scheme 2.

Conclusion

We have demonstrated here that bichromophoric 1-(arylmethyloxy)-2-pyridones having a strong ability to form an intramolecular exciplex undergo novel photo-induced heterolytic cleavage of the C–O bond, in competition with the N–O bond homolysis. There was a great difference in the relative composition of the heterolytic bond-cleavage products between the bichromophoric 1-hydroxy-2-pyridone derivatives carrying 9-anthrylmethyl and pyren-1-ylmethyl groups. Because the reduction ability of the 9-anthrylmethyl radical is considered to be very similar to that of the pyren-1-ylmethyl,[4,11] we have only a very small contribution of the mechanism in which the arylmethylcarbonium ion is formed by homolytic scission of the C–O bond within a singlet-exciplex intermediate, followed by electron transfer from the arylmethyl radical to the 2-pyridone-1-oxyl.

Experimental

Materials and solvents

1-(9-Anthrylmethyloxy)-2-pyridone (**1a**) was prepared by the reaction of 1-hydroxy-2-pyridone (Aldrich) with 9-(chloromethyl)anthracene (Aldrich) in dimethyl sulfoxide (DMSO) containing 1,8-diazabicyclo[5.4.0]undec-7-ene (DBU) at 110 °C. The reaction of 2-methoxy-6-methylpyridine *N*-oxide with 9-(chloromethyl)anthracene in refluxing toluene afforded 1-(9-anthrylmethyloxy)-6-methyl-2-pyridone (**1b**). The former reagent was prepared by the oxidation of 2-chloro-6-methylpyridine with *m*-chloroperbenzoic acid in chloroform, followed by the methoxylation of 2-chloro-6-methylpyridine *N*-oxide with sodium methoxide in methanol. The synthesis of 1-(pyren-1-ylmethyloxy)-2-pyridone (**1c**) was accomplished by treatment of 1-(chloromethyl)pyrene, obtained by the reaction between pyrene-1-methanol and thionyl chloride in pyridine–isopropyl ether, with 1-hydroxy-2-pyridone in DMSO–DBU at 110 °C. Pyrene-1-methanol was synthesized by the reduction of pyrene-1-carbaldehyde (Aldrich) with sodium borohydride in chloroform–ethanol (10 : 1 v/v). The crude products **1a**, **1b** and **1c** were purified by column chromatography over silica gel (70–230 mesh, Merck) using ethyl acetate–hexane as the eluent. The reaction of sodium methoxide with 9-(chloromethyl)-anthracene and 1-(chloromethyl)pyrene in methanol allowed us to obtain crude 9-(methoxymethyl)anthracene (**6a**) and 1-(methoxymethyl)pyrene (**6c**), respectively, which were subjected to column chromatography over silica gel (70–230 mesh, Merck) using chloroform–hexane as the eluent. Treatment of 9-(chloromethyl)anthracene with sodium ethoxide in ethanol gave 9-(ethoxymethyl)anthracene (**7**) which was purified according to the method described above. The physical and spectroscopic properties of these compounds are as follows.

1a, mp 174.0–175.0 °C; ν_{max} (KBr)/cm^{-1} 1660; δ_H (500 MHz; $CDCl_3$) 5.72 (1H, ddd, *J* 1.8, 6.7 and 7.0), 6.38 (2H, s), 6.70 (1H, dd, *J* 1.8 and 9.2), 6.91 (1H, dd, *J* 1.8 and 7.0), 7.16 (1H, ddd, *J* 1.8, 6.7 and 9.2), 7.48 (2H, dd, *J* 6.7 and 8.6), 7.58 (2H, dd, *J* 6.7 and 8.9), 8.01 (2H, d, *J* 8.6), 8.51 (1H, s) and 8.51 (2H, d, *J* 8.5); δ_C ($CDCl_3$) 70.1, 104.8, 122.6, 123.8 (2C), 124.1, 125.3 (2C), 127.2 (2C), 129.1 (2C), 130.1 (2C), 131.2, 132.0 (2C), 136.5, 138.8 and 159.4 (Found: C, 79.4; H, 4.9; N, 4.6%. $C_{20}H_{15}NO_2$ requires C, 79.7; H, 5.0; N, 4.65%).

1b, mp 122.0–123.0 °C; ν_{max} (KBr)/cm^{-1} 1670; δ_H (500 MHz; $CDCl_3$) 2.06 (3H, s), 5.84 (1H, d, *J* 6.7), 6.39 (2H, s), 6.64 (1H, d, *J* 9.2), 7.19 (1H, dd, *J* 6.7 and 9.2), 7.47 (2H, dd, *J* 7.3 and 7.9), 7.61 (2H, dd, *J* 7.3 and 9.2), 8.03 (2H, d, *J* 7.9), 8.54 (1H, s) and 8.71 (2H, d, *J* 9.2); δ_C ($CDCl_3$) 17.3, 69.3, 105.2, 119.5 (2C), 124.2 (2C), 125.0, 125.2 (2C), 127.1 (2C), 129.0 (2C), 130.0, 131.7, 132.0 (2C), 138.4, 146.6 and 160.4 (Found: C, 79.8; H, 5.2; N, 4.2%. $C_{21}H_{17}NO_2$ requires C, 80.0; H, 5.4; N, 4.4%).

1c, mp 114.0–115.0 °C; ν_{max} (KBr)/cm^{-1} 1650; δ_H (500 MHz; $CDCl_3$) 5.65 (1H, ddd, *J* 1.2, 6.7 and 7.0), 6.03 (2H, s), 6.72 (1H, dd, *J* 1.2 and 9.2), 6.85 (1H, dd, *J* 1.8 and 7.0), 7.17 (1H, ddd, *J* 1.8, 6.7 and 9.2), 7.90 (1H, d, *J* 7.9), 8.02 (1H, d, *J* 8.5), 8.04 (1H, dd, *J* 7.9 and 8.5), 8.07 (1H, d, *J* 7.9), 8.09 (1H, d,

J 8.5), 8.21 (1H, d, *J* 7.9), 8.22 (1H, d, *J* 9.2), 8.24 (1H, d, *J* 8.5) and 8.66 (1H, d, *J* 9.2); δ_C ($CDCl_3$) 76.2, 104.4, 122.6, 123.3, 124.5, 124.8, 125.7 (2C), 125.8 (2C), 126.2, 126.7, 127.3, 128.3, 128.8, 129.3, 130.7, 131.1, 132.5, 136.6, 138.6 and 159.2 (Found: C, 81.1; H, 4.7; N, 4.2%. $C_{22}H_{15}NO_2$ requires C, 81.2; H, 4.65; N, 4.3%).

6a, mp 87.5–89.0 °C; ν_{max} (KBr)/cm^{-1} 1190; δ_H (500 MHz; $CDCl_3$) 3.55 (3H, s), 5.44 (2H, s), 7.47 (2H, dd, *J* 6.4 and 8.5), 7.55 (2H, dd, *J* 6.4 and 8.5), 8.02 (2H, d, *J* 8.5), 8.39 (2H, d, *J* 8.5) and 8.47 (1H, s); δ_C ($CDCl_3$) 58.4, 66.6, 124.3 (2C), 125.0 (2C), 126.2 (2C), 128.4, 129.0 (2C), 131.0 (2C), 131.5 (2C) and 134.1 (Found: C, 86.3; H, 6.2%. $C_{16}H_{14}O$ requires C, 86.45; H, 6.35%).

6c, mp 52.5–54.0 °C; ν_{max} (KBr)/cm^{-1} 1086; δ_H (500 MHz; $CDCl_3$) 3.50 (3H, s), 5.15 (2H, s), 7.98 (1H, dd, *J* 7.3 and 7.3), 8.00 (1H, d, *J* 7.9), 8.03 (2H, br s), 8.12 (1H, d, *J* 9.2), 8.12 (1H, d, *J* 7.9), 8.16 (1H, d, *J* 7.3), 8.17 (1H, d, *J* 7.3) and 8.33 (1H, d, *J* 9.2); δ_C ($CDCl_3$) 58.2, 73.2, 123.3, 124.5, 124.7, 124.9, 125.2 (2C), 125.9, 127.0, 127.4 (2C), 127.7 (2C), 129.3, 130.8, 131.2 and 131.3 (Found: C, 87.5; H, 5.7%. $C_{18}H_{14}O$ requires C, 87.8; H, 5.7%).

7, mp 76.5–77.5 °C; ν_{max} (KBr)/cm^{-1} 1089; δ_H (500 MHz; $CDCl_3$) 1.28 (3H, t, *J* 7.0), 3.75 (2H, q, *J* 7.0), 5.47 (2H, s), 7.46 (2H, dd, *J* 6.6 and 8.6), 7.54 (2H, dd, *J* 6.6 and 8.9), 8.00 (2H, d, *J* 8.6), 8.39 (2H, d, *J* 8.9) and 8.45 (1H, s); δ_C ($CDCl_3$) 15.4, 64.8, 66.0, 124.4 (2C), 124.9 (2C), 126.1, 128.3 (2C), 129.01 (2C), 129.04, 131.0 (2C) and 131.5 (2C) (Found: C, 86.2; H, 6.6%. $C_{17}H_{16}O$ requires C, 86.4; H, 6.8%).

1-Hydroxy-2-pyridone (**2a**), 2-pyridone (**3a**), anthracene-9-methanol (**4a**), pyrene-1-methanol (**4c**), anthracene-9-carbaldehyde (**5a**) and pyrene-1-carbaldehyde (**5c**) were recrystallized from ethyl acetate–hexane or reprecipitated with hexane. Pyrene (optical grade, Aldrich) and anthracene (zone-refined, Aldrich) were used without further purification. Methanol and ethanol were purified according to standard methods.[12] All other chemicals employed were obtained from commercial sources and were of the highest grade available.

Measurements

UV absorption and fluorescence spectra were recorded on a Shimadzu UV-2200 spectrophotometer and a Shimadzu RF-5000 spectrofluorimeter, respectively. HPLC analyses of the photoproducts were performed on a Shimadzu Model LC-6A high-performance liquid chromatography system equipped with a 4.6 × 250 mm ODS (Zorbax) column and a Shimadzu Model SPD-2A UV detector (detection wavelength, 240 nm; mobile phase, MeCN–H_2O = 60 : 40 v/v). Linear calibration curves for each compound, obtained under the same analytical conditions, were utilized to quantify the appearance of the products. ^1H and ^{13}C NMR spectra were taken with a JEOL JNM-A500 spectrometer. Chemical shifts (in ppm) were determined using tetramethylsilane as an internal standard. *J* values are given in Hz. NOESY spectra were recorded with a spectral width of 5283 Hz. The 90° pulse was 12.4 μs, mixing time was 500 ms, delay time was 2.4 s and 1024 × 1024 data points were recorded. Fluorescence lifetimes of anthracene and pyrene were measured under nitrogen with a time-correlated single-photon counting apparatus (Horiba NAES-700; excitation wavelength, 342 nm; cut-off wavelength, 380 nm), which was equipped with a flash lamp filled with hydrogen. Ten thousand counts were sampled in the peak channel. IR spectra were taken with a Hitachi Model 270-30 infrared spectrometer.

A potassium tris(oxalato)ferrate(III) actinometer was employed to determine the quantum yields for the appearance of **4**–**6** at low conversions of the starting hydroxylamine **1** (10–15%).[10] A 450 W high-pressure Hg lamp was used as the light source from which 366 nm light was selected with Corning 0-52, Corning 7-60 and Toshiba IRA-25S glass filters. All of the quantum yields are an average of more than five determinations.

In order to examine the irradiation time dependence of the product composition, a methanol solution (100 mL) of **1** ([**1a**], 1.0×10^{-3}; [**1c**], 5.0×10^{-4} mol dm^{-3}), placed in a Pyrex vessel, was irradiated with light of wavelength longer than 340 nm (from a 450 W high-pressure Hg lamp) under nitrogen at room temperature. At suitable time intervals, an aliquot (10 mL) of the solution was pipetted off and concentrated to dryness *in vacuo*. The resulting residue was dissolved in $CDCl_3$ and subjected to ^1H NMR analysis. The composition was estimated from the area ratio of a given ^1H NMR signal for each compound. The remaining solution of **1a** was concentrated to dryness under reduced pressure and the resulting residue was subjected to preparative thin layer chromatography over silica gel (eluent: ethyl acetate–hexane) to isolate **2a**, **3a** and **6a**.

Acknowledgements

This research was partially supported by a "High-Tech Research Center Project" from the Ministry of Education, Culture, Sports, Science and Technology, Japan.

References

1 R. W. Binkly and T. W. Flechtner, in *Synthetic Organic Photochemistry*, ed. W. M. Horspool, Plenum Press, New York, 1984, pp. 375–423.
2 Y. Shi, J. E. T. Corrie and P. Wan, *J. Org. Chem.*, 1997, **62**, 8278 and references cited therein.
3 (*a*) S. A. MacDonald, C. G. Willson and J. M. J. Fréchet, *Acc. Chem. Res.*, 1994, **27**, 151; (*b*) M. C. Pirrung and C.-Y. Huang, *Tetrahedron Lett.*, 1995, **36**, 5883; (*c*) J. F. Cameron, C. G. Willson and J. M. J. Fréchet, *J. Am. Chem. Soc.*, 1996, **118**, 12 925.
4 (*a*) J. A. Pincock, *Acc. Chem. Res.*, 1997, **30**, 43; (*b*) S. M. Nevill and J. A. Pincock, *Can. J. Chem.*, 1997, **75**, 232; (*c*) F. L. Cozens, A. L. Pincock, J. A. Pincock and R. Smith, *J. Org. Chem.*, 1998, **63**, 434; (*d*) D. P. DeCosta, A. Bennett, A. L. Pincock, J. A. Pincock and R. Stefanova, *J. Org. Chem.*, 2000, **65**, 4162; (*e*) D. P. DeCosta, N. Howell, A. L. Pincock, J. A. Pincock and S. Rifai, *J. Org. Chem.*, 2000, **65**, 4698.
5 (*a*) J. Dreyer and K. S. Peters, *J. Phys. Chem.*, 1996, **100**, 15 156 and references cited therein; (*b*) J. Dreyer, M. Lipson and K. S. Peters, *J. Phys. Chem.*, 1996, **100**, 15 162.
6 T. Sakurai, Y. Takeda and H. Inoue, *Nippon Kagaku Kaishi*, 1984, 1.
7 (*a*) T. Sakurai, T. Obana, T. Inagaki and H. Inoue, *J. Chem. Soc., Perkin Trans. 2*, 1989, 535; (*b*) T. Sakurai, Y. Murakata and H. Inoue, *J. Chem. Soc., Perkin Trans. 2*, 1990, 499.
8 S. L. Murov, I. Carmichael and G. L. Hug, *Handbook of Photochemistry*, 2nd edn., Marcel Dekker, New York, 1993.
9 (*a*) H.-D. Becker, C. Burgdorff and H.-G. Löhmannsröben, *J. Photochem. Photobiol. A: Chem.*, 1995, **86**, 133; (*b*) C. Burgdorff, H.-G. Löhmannsröben and T. Sander, *J. Chem. Soc., Faraday Trans.*, 1996, **92**, 3043.
10 C. G. Hatchard and C. A. Parker, *Proc. R. Soc. London, Ser. A*, 1956, **235**, 518.
11 G. J. Kavarnos and N. J. Turro, *Chem. Rev.*, 1986, **86**, 401.
12 J. A. Riddick, W. B. Bunger and T. K. Sakano, *Organic Solvents*, 4th edn., Wiley, Chichester, 1986.